Acta Pharmacologica Sinica

www.nature.com/aps

ARTICLE

# A novel derivative of valepotriate inhibits the PI3K/AKT pathway and causes Noxa-dependent apoptosis in human pancreatic cancer cells

You-you Yan[1,2], Ke-yu Shi[1,2,3], Fei Teng[1,2,3], Jing Chen[3], Jin-xin Che[4], Xiao-wu Dong[4], Neng-ming Lin[1,2,3] and Bo Zhang[1,2]

Natural compound valepotriate exhibits inhibitory activity against a number of cancers, but the effect of valepotriate against pancreatic cancer is unclear, and the structure–activity relationship of valepotriate has not been characterized. In this study, we performed a structure-based similarity search and found 16 hit compounds. Among the 16 hits, (1S,6S,7R)-6-(acetyloxy)-1-[(3-methylbutanoyl)oxy]-4a,5,6,7a-tetrahydro-1H-spiro[cyclopenta[c]pyran-7,2′-oxiran]-4-ylmethyl 3-methylbutanoate (denoted as Amcp) exhibited superior anticancer activity against human pancreatic cancer BxPC-3 and SW1990 cells. The anti-proliferation activity of Amcp was validated in human pancreatic cancer BxPC-3 and SW1990 cells in vitro. Amcp more effectively induced apoptosis in BxPC-3 and SW1990 cells than gemcitabine. At a concentration of 15 μM, Amcp significantly suppressed the PI3K/AKT pathway and disrupted the mitochondrial membrane equilibrium through modulation of Noxa and Mcl-1 balance in both cell lines. Meanwhile, knockdown of Noxa substantially attenuated Amcp-induced reduction of cell viability and anti-apoptotic protein Mcl-1 level in BxPC-3 cells. In addition, Amcp showed synergistic anticancer effects when combined with gemcitabine in BxPC-3 cells. To conclude, this work not only suggests that Amcp possesses a dual-inhibitory activity towards PI3K/AKT pathway and Mcl-1, but also enlightens further development of bioactive valepotriate derivatives.

**Keywords:** valepotriate; human pancreatic cancer; PI3K/AKT; Noxa; Mcl-1

*Acta Pharmacologica Sinica* (2020) 41:835–842; https://doi.org/10.1038/s41401-019-0354-1

## INTRODUCTION

Pancreatic ductal adenocarcinoma (PDAC) is an aggressive malignancy and is predicted to be the second leading cause of cancer-related mortality in the near future [1]. Systemic chemotherapy is an important part of treatment for PDAC patients, especially those who are diagnosed at advanced stages. Although great efforts have been made to explore efficacious compounds for treating PDAC in both preclinical and clinical studies, the 5-year survival rate remains at ~5% and has not changed for the past 30 years [2]. Gemcitabine has been a key component of gold standard chemotherapy regimens for pancreatic cancer, but the actual clinical response rate to gemcitabine has been unsatisfactory. It was reported that the phosphoinositide 3-kinase (PI3K)/AKT signaling pathway was aberrantly activated in most pancreatic cancer patients [3] and the concomitant inhibition of PI3K/AKT and Mcl-1 was considered to be a promising strategy to inhibit the progression of pancreatic cancer [4–6]. In addition, Noxa is a BH-3 domain-containing protein that is capable of binding and sequestering pro-survival Bcl-2 family proteins such as Mcl-1 and Bcl-2, and therefore the downregulation of Mcl-1 via Noxa activation is considered to be an efficacious therapeutic strategy for a variety of cancers [7, 8]. Unfortunately, most clinical tests of revised chemotherapy regimens have failed, probably due to the complexity of pancreatic cancer [9]. Therefore, novel chemotherapeutic agents are still urgently needed to combat this aggressive neoplasm.

Valeriana is a natural medicinal herb, for which the root extracts have been extensively studied in many aspects as part of anticancer, anti-bacterial, and anti-anxiety investigations [10–12]. Valepotriate is the key bioactive component extracted from Valeriana and is reported to exert anti-proliferation cytotoxic effects by regulating the redox balance or suppressing the mitogen-activated protein kinase pathway in cancer cells [13, 14]. However, the anticancer activity of valepotriate against pancreatic cancer has been rarely shown in the last few decades. In addition, it remains unclear whether the structure–activity relationship of valepotriate is unique. Therefore, extensive work and deeper exploration are required to fully investigate valepotriate and its derivatives as anticancer agents.

Herein, we obtained a series of valepotriate derivatives and aimed to explore candidate compounds with potent anticancer activity against pancreatic cancer cells. By using a structure-based

[1]Department of Clinical Pharmacology, Key Laboratory of Clinical Cancer Pharmacology and Toxicology Research of Zhejiang Province, Hangzhou First People's Hospital, Zhejiang Chinese Medical University, Hangzhou 310006, China; [2]Translational Medicine Research Center, Affiliated Hangzhou First People's Hospital, Zhejiang University School of Medicine, Hangzhou 310006, China; [3]College of Pharmaceutical Sciences, Zhejiang Chinese Medical University, Hangzhou 311402, China and [4]ZJU-ENS Joint Laboratory of Medicinal Chemistry, Zhejiang Province Key Laboratory of Anti-Cancer Drug Research, College of Pharmaceutical Sciences, Zhejiang University, Hangzhou 310058, China
Correspondence: Neng-ming Lin (lnm1013@zju.edu.cn) or Bo Zhang (zhangbohzss@163.com)
These authors contributed equally: You-you Yan, Ke-yu Shi, Fei Teng

Received: 2 September 2019 Accepted: 29 December 2019
Published online: 11 February 2020

© CPS and SIMM 2020

similarity search, we identified 16 compounds that had similar backbones but differed in terms of their substitution groups. Among these compounds, (1S,6S,7R)-6-(acetyloxy)-1-[(3-methylbutanoyl)oxy]-4a,5,6,7a-tetrahydro-1H-spiro [cyclopenta[c]pyran-7,2′-oxiran]-4-ylmethyl 3-methylbutanoate (denoted as Amcp) was chosen for the following experiments and its mechanisms of action were validated.

## MATERIALS AND METHODS

### Cell culture

RPMI-1640 medium and fetal bovine serum (FBS) were purchased from Gibco (Grand Island, NY, USA). DAPI (4′,6-diamidino-2-phenylindole) was purchased from Wuhan Goodbio Technology Co., Ltd (Wuhan, China). The Annexin V-FITC Apoptosis Kit was purchased from BestBio (Shanghai, China). The Mitochondrial Membrane Potential Assay Kit was purchased from Signalway Antibody (College Park, MD, USA). The primary antibodies against poly(ADP-ribose) polymerase (PARP), caspase-3, cleaved caspase-3, PI3K-p110α, p-AKT (Ser 473), AKT, mammalian target of rapamycin (mTOR), p-mTOR (S2448), p-p70S6, p70S6, p-S6 (240/244), p-S6 (235/236), S6, and Bcl-2 were purchased from Cell Signaling Technology (Beverly, MA, USA). The primary antibodies against X-linked inhibitor of apoptosis protein (XIAP), Bax, Noxa, Bcl-XL, Mcl-1, and β-actin were purchased from Abcam, Inc. (Cambridge, MA, USA). The human pancreatic cancer cell lines BxPC-3 (Catalog Number TCHu12) and SW1990 (Catalog Number TCHu201) were purchased from the Chinese Academy of Sciences (Shanghai, China). Cells were cultured in RPMI-1640 medium containing 10% FBS and 100 U/mL penicillin/streptomycin at 37 °C in 5% $CO_2$ in a humidified atmosphere. Amcp was dissolved in dimethyl sulfoxide (DMSO) at a concentration of 10 mM. Gemcitabine was dissolved in DMSO at a concentration of 10 mM.

### Similarity search

The structure-based similarity search was performed using the Structure Search plugin on the MolPort website (https://www.molport.com/shop/find-chemicals). (1R)-2,6,7,7a-tetrahydrospiro [indene-1,2′-oxirane] was used as the initial structure. The similarity value was set to 0.6. After searching, 16 compounds were chosen and purchased from Targetmol (Shanghai, China).

### Cell viability assay

Cell proliferation was measured by using a cell counting kit-8 (CCK-8) assay (Bestbio, Shanghai, China). Cells were cultured in 96-well plates at a concentration of $5 \times 10^3$–$7 \times 10^3$/well. Cells were cultured for 24 h and treated with 0.625, 1.25, 2.5, 5, and 10 μM Amcp. After 24, 48, or 72 h of treatment, the supernatant was completely removed and 100 μL of CCK-8 solution was added to each well, and the cells were cultured for another 2 h at 37 °C. Cell viability was quantified by a SpectraMax M3e instrument (Molecular Devices, San Jose, CA, USA) at 450 nm. Cell viability was calculated for each well using the formula $OD_{450}$ treated cells/$OD_{450}$ control cells × 100%. Assays were performed in three independent experiments.

### DAPI staining

BxPC-3 or SW1990 cells ($8 \times 10^4$ cells/well) were cultured in 24-well plates. After exposure to Amcp or gemcitabine for 24 h, the cells were fixed with 4% paraformaldehyde for 20 min and stained with DAPI for 15 min. After washing with phosphate-buffered saline (PBS), the cells were observed under a fluorescence microscope (Nikon, Ti-E, Japan).

### Apoptosis assay

Cells in the exponential growth phase were seeded in six-well plates ($2 \times 0^5$/well) and cultured overnight in a 5% $CO_2$ atmosphere at 37 °C. After treatment with Amcp or gemcitabine for 24 h, the cells were collected and washed with PBS. Then, cells were stained with an Annexin V-FITC Apoptosis Kit according to the manufacturer's instructions and analyzed by flow cytometry (Becton Dickinson, Franklin Lakes, NJ, USA). Assays were performed in three independent experiments.

### Detection of the mitochondrial membrane potential

The mitochondrial membrane potential was visualized by 5,5′,6,6′-tetrachloro-1,1′,3,3′ tetraethyl-imidacarbocyanine iodide (JC-1) staining. Cells were seeded into six-well plates at a density of $2 \times 10^5$/well and cultured for 24 h. After 12 h of treatment, the cells were collected, washed with PBS, and incubated with JC-1 for 15 min at 37 °C. After washing off the dye, the cells were immediately analyzed using flow cytometry (Becton Dickinson, Franklin Lakes, NJ, USA). Assays were performed in three independent experiments.

### Noxa transient siRNA knockdown

Small interfering RNAs (siRNAs) targeting Noxa [Noxa-Homo1 (siRNA-1), Noxa-Homo2 (siRNA-2), Noxa-Homo3 (siRNA-3)], and control siRNA (siControl) were purchased from Guannan Co. Ltd. (Hangzhou, China). The target sequences were as follows:

| | |
|---|---|
| siRNA-1 | 5′-UGGAAGUCGAGUGUGCUACUCTT-3′ |
| siRNA-2 | 5′-GCAGAAACUUCUGAAUCUGAUTT-3′ |
| siRNA-3 | 5′-GCAUUGUUGUUGUUGCUGUUUTT-3′ |
| siControl | 5′-UUCUCCGAACGUGUCACGUTT-3′ |

Transient transfection of BxPC-3 cells was performed using 20 μM of each siRNA with Lipofectamine 2000 (Invitrogen, Carlsbad, CA, USA). Knockdown of Nova was verified by real-time quantitative reverse-transcriptase PCR.

### Western blotting analysis

After cells were treated with different concentrations of Amcp or gemcitabine, the total proteins were extracted using RIPA lysis buffer. A total of 40 μg of protein was subjected to 12% SDS-polyacrylamide gel electrophoresis and transferred to polyvinylidene difluoride membranes (Bio-Rad, Hercules, CA, USA). The membranes were blocked with 5% non-fat milk at room temperature for 1 h and then incubated with specific primary antibodies (1:500–1:1000 dilution) overnight at 4 °C. After washing with Tris-buffered saline and Tween 20, the membranes were incubated with secondary antibodies (1:5000 dilution) at room temperature for another 1 h. The protein bands were visualized by adding the ECL reagent WBKLS0050 (EMD Millipore, Billerica, MA, USA) and analyzed using Bio-Rad Laboratories Quantity One software (Bio-Rad, Hercules, CA, USA).

### Statistical analyses

Statistical analysis was performed in GraphPad Prism 5. A two-sided Student's *t*-test or one-way analysis of variance was used to analyze the differences among groups. The results are expressed as the mean ± SD of at least three independent experiments. A *P*-value < 0.05 was considered statistically significant.

## RESULTS

### Amcp induced apoptosis in BxPC-3 and SW1990 cells

A similarity search was employed to find derivatives of valepotriate that were potentially active against cancer cells and the results identified 16 hit compounds that were purchased for bioactivity tests. Examples of five of the hit compounds are shown in Fig. 1. Among the 16 compounds, Amcp (Fig. 2a) exhibited superior anticancer activity compared with the other compounds

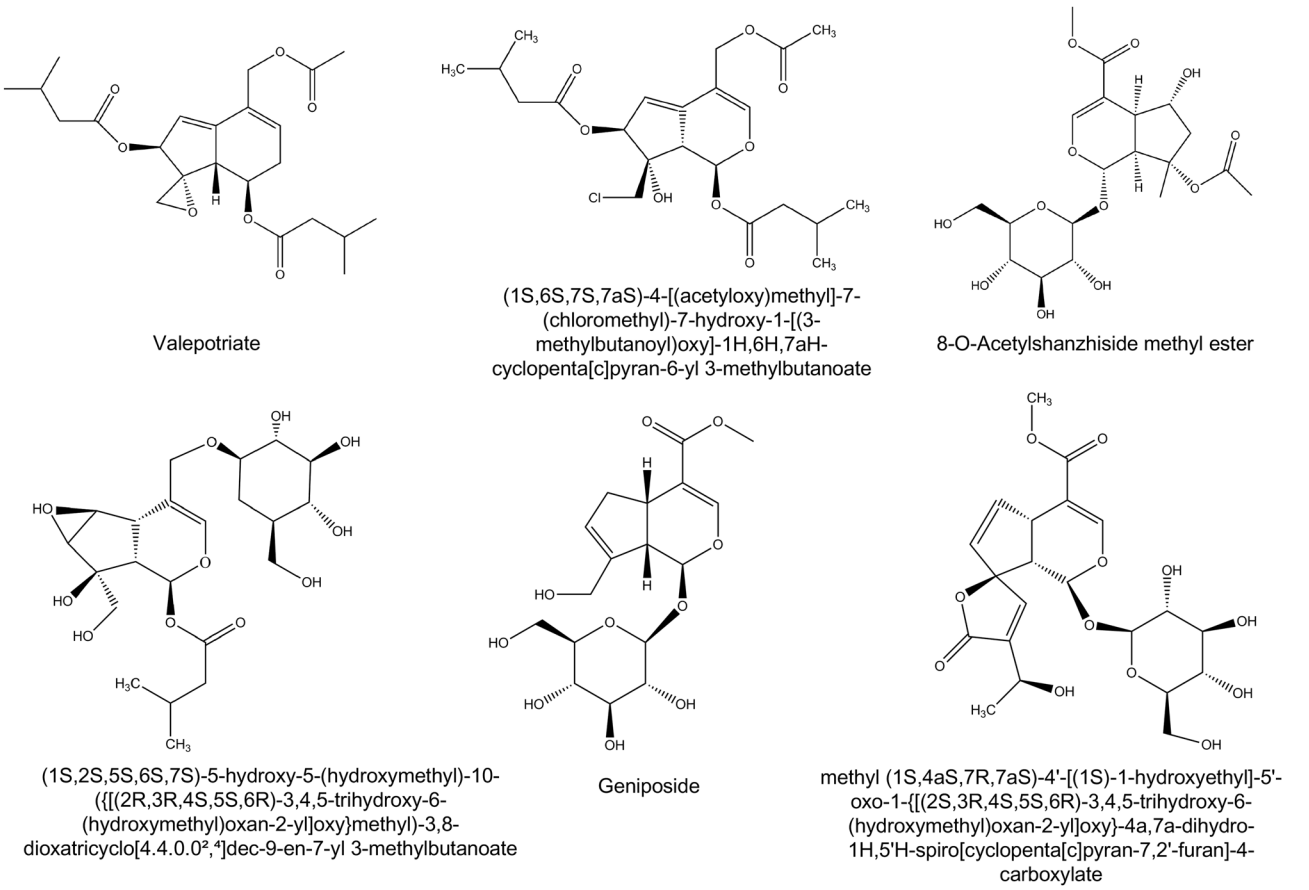


**Fig. 1 Chemical structures of valepotriate and 5 hit compounds.** Examples of five hit compounds obtained through a similarity search using (1R)-2,6,7,7a-tetrahydrospiro[indene-1,2′-oxirane] as the initial structure.

in both BxPC-3 and SW1990 cells. To verify the anti-proliferation effects of Amcp, both BxPC-3 and SW1990 cells were incubated with the indicated concentrations of Amcp for the indicated times, as shown in Fig. 2b. As a result, Amcp produced a concentration- and time-dependent inhibitory effect against both BxPC-3 and SW1990 cells. In addition, gemcitabine, which is considered the standard single chemotherapeutic agent in the clinic, was used as a positive control to verify the effects against pancreatic cancer cells. By using DAPI staining, shrunken cell nuclei and reduced cell numbers were observed after treatment with increasing concentrations of Amcp. At a concentration of 15 μM, Amcp was more efficacious in inhibiting the proliferation of pancreatic cancer cells than gemcitabine (Fig. 2c).

To demonstrate that the anti-proliferation effect of Amcp was attributed to the induction of apoptosis, cells were stained with Annexin V/propidium iodide and analyzed by flow cytometry. As shown in Fig. 3a, Amcp dose-dependently induced both early and late apoptosis in BxPC-3 and SW1990 cells. At a concentration of 15 μM, Amcp significantly increased the number of apoptotic cells compared with gemcitabine in both cell lines (Fig. 3b). In addition, Western blotting was applied to determine the proteins involved in the regulation of the occurrence of apoptosis. An increase in cleaved caspase-3 and the appearance of cleaved PARP after treatment with 15 μM Amcp suggested the occurrence of caspase-dependent apoptosis (Fig. 3c). Moreover, BxPC-3 and SW1990 cells were pretreated with the caspase paninhibitor Z-VAD-FMK for 2 h before culturing them with the indicated concentrations of Amcp (Fig. 4a). The addition of Z-VAD-FMK substantially reversed the inhibitory effects of Amcp on BxPC-3 and SW1990 cells, and reduced the downregulation of caspase-3, indicating that caspase-dependent apoptosis played a critical role in the anti-proliferation effects of Amcp (Fig. 4b).

### Amcp selectively suppressed the activation of the PI3K/AKT pathway and disrupted the mitochondrial membrane potential

Aberrant activation of PI3K pathways is commonly found in many pancreatic cancer patients, indicating a need for the development of novel compounds targeting these key regulators of the PI3K pathway [15]. We therefore intended to explore the effects of Amcp on the PI3K pathway. Amcp substantially suppressed the phosphorylation of AKT and mTOR, and slightly affected their total protein levels (Fig. 4c). In contrast, treatment with gemcitabine scarcely affected the phosphorylation of proteins in the PI3K/AKT pathway, thus highlighting the unique mechanisms of action of Amcp. As the disruption of the PI3K/AKT pathway causes mitochondrial instability [16], we detected the mitochondrial membrane potential after exposure to Amcp. As expected, cells treated with Amcp exhibited a substantial decrease in the mitochondrial membrane potential, which was significantly more severe than that in cells treated with gemcitabine (Fig. 5a, b). In addition, proteins that play major roles in regulating the mitochondrial membrane potential were analyzed by Western blotting (Fig. 5c). It is worth mentioning that the anti-apoptotic protein Mcl-1 was obviously downregulated in both cell lines after Amcp treatment, whereas Noxa was apparently upregulated by 15 μM Amcp treatment.

### Noxa-dependent Mcl-1 downregulation was critical for Amcp-induced apoptosis

It has been reported that Noxa can act as an E3 ligase and mediate the degradation of Mcl-1 under certain circumstances [17].

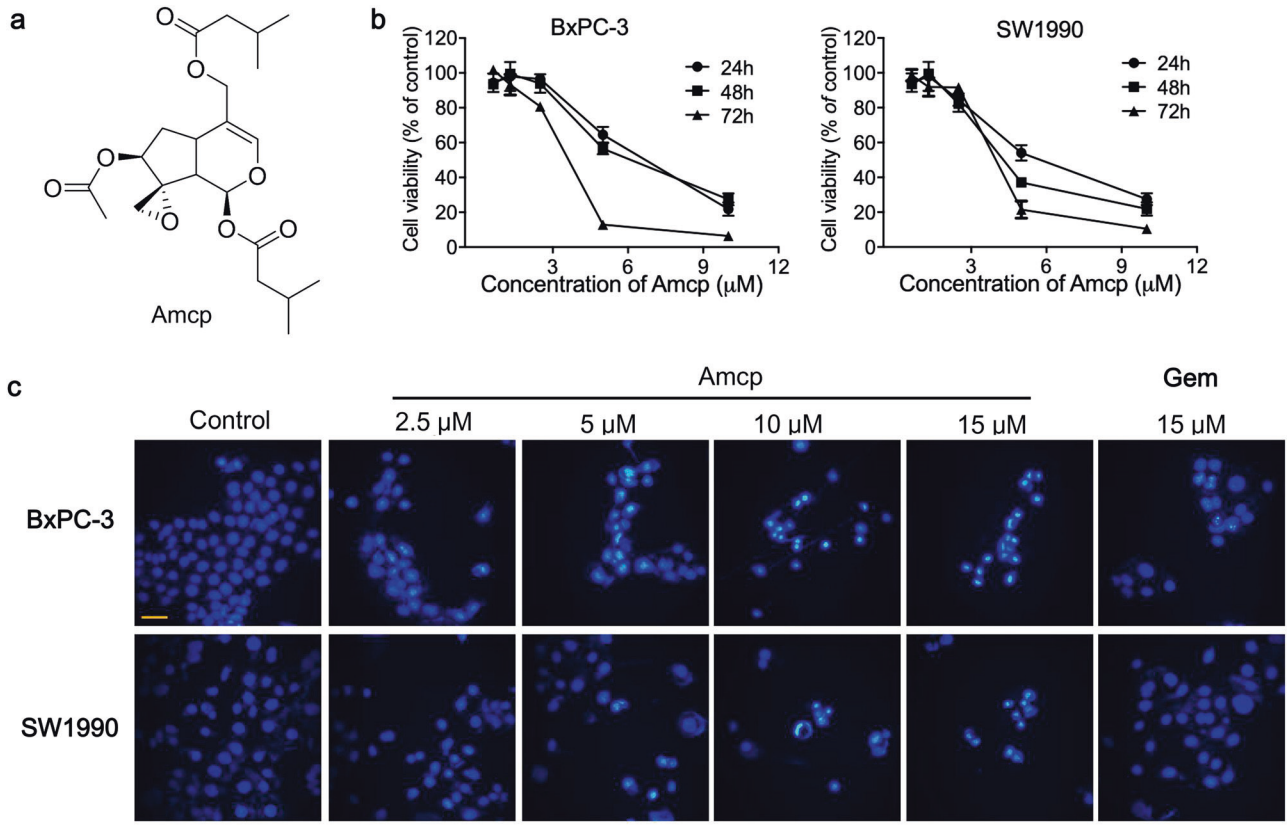


**Fig. 2 Amcp inhibited the proliferation of human pancreatic cancer cells. a** The chemical structure of Amcp. **b** The time- and dose-dependent inhibitory effects of Amcp on two human pancreatic cancer cell lines, BxPC-3 and SW1990, in vitro. Cells were treated with Amcp at concentrations of 0.625, 1.25, 2.5, 5, and 10 μM for either 24, 48, or 72 h before the CCK-8 assay. **c** DAPI staining of the cell nucleus. Cells were treated with the indicated compounds for 24 h before fixation and stained with DAPI stain. Fluorescence was observed by using microscopy (Nikon Eclipse Ti). The magnification is ×400. Scale bar = 20 μm.

Therefore, we aimed to determine the role of Noxa in Amcp-induced apoptosis. Noxa was successfully knocked down by customized siRNA interference in BxPC-3 cells (Fig. 5d) and siRNA #2 was used for the following experiments. After knocking down Noxa, the number of viable cells significantly increased from ~25% to 48% during exposure to 15 μM Amcp (Fig. 5e). In addition, Amcp-induced apoptosis was apparently attenuated after Noxa knockdown, indicating increased levels of caspase-3 and PARP (Fig. 5f). Meanwhile, the decrease in the protein levels of both Mcl-1 and Bcl-2 caused by Amcp was obviously reversed by knocking down Noxa, suggesting that Noxa is a key protein involved in regulating Mcl-1. In addition, cycloheximide was used to pretreat cells for 0.5 h to explore the degradation dynamics of Mcl-1 in cells with or without Amcp. Interestingly, Amcp obviously accelerated the degradation of Mcl-1 after 4 or 8 h of treatment (Fig. 5g).

Synergistic effects of Amcp with gemcitabine in BxPC-3 cells

It was shown that Amcp exhibited potent anticancer activity against pancreatic cancer cells as a single agent. In addition, Amcp displayed a synergistic effect when used in combinatorial treatment with gemcitabine in BxPC-3 cells. Both 2.5 and 5.0 μM Amcp significantly enhanced the cytotoxicity of gemcitabine (Fig. 6a). Combinatorial treatment with Amcp and gemcitabine synergistically induced apoptosis in BxPC-3 cells (Fig. 6b, d) and this effect could be partially overcome by the addition of the pancaspase inhibitor Z-VAD-FMK (Fig. 6c). Furthermore, depolarization of the mitochondrial membrane was found to be significantly increased after combination treatment with Amcp and gemcitabine, suggesting that mitochondrion-dependent apoptosis might play a pivotal role in this event (Fig. 6e).

## DISCUSSION

Iridoids isolated from Valeriana have recently been reported to possess various biological activities, including anticancer effects [18–20]. However, large numbers of bioactive iridoids remain to be identified and their structure–activity relationships still need to be validated. In this study, we identified a series of valepotriate derivatives through a similarity search. During the initial anti-proliferative activity screening, Amcp exhibited a potent anticancer activity against pancreatic cancer cells in vitro and was therefore chosen for the following experiments. As caspases are frequently cleaved into active components once they are activated by various cellular stimuli, we examined the protein expression of both pro- and cleaved caspase-3, and the proteolytic cleavage of PARP [21, 22]. As shown in Fig. 3, the expression of activated caspase-3 was significantly upregulated and the expression of PARP was diminished after Amcp exposure, suggesting that Amcp induced caspase-3-mediated apoptosis in a concentration-dependent manner [23]. In addition, the protein expression of XIAP was gradually decreased and active caspase-3 could be detected (Fig. 3c). It was reported that XIAP is an inhibitor of apoptosis that represses the activation of caspase-3 and 9; on the other hand, XIAP activity could be attenuated by caspase-3 during the inhibition of caspase-9 [24, 25]. We also found that pretreatment with the pancaspase inhibitor Z-VAD-FMK significantly reversed Amcp-induced proliferation suppression in both BxPC-3 and SW1990 cells (Fig. 3d). Taken together, the results showed that the activation of caspase-3 played an essential role in Amcp-induced apoptosis in pancreatic cancer cells.

The PI3K/AKT signaling pathway is commonly activated in many human cancers, including pancreatic cancer, and S473

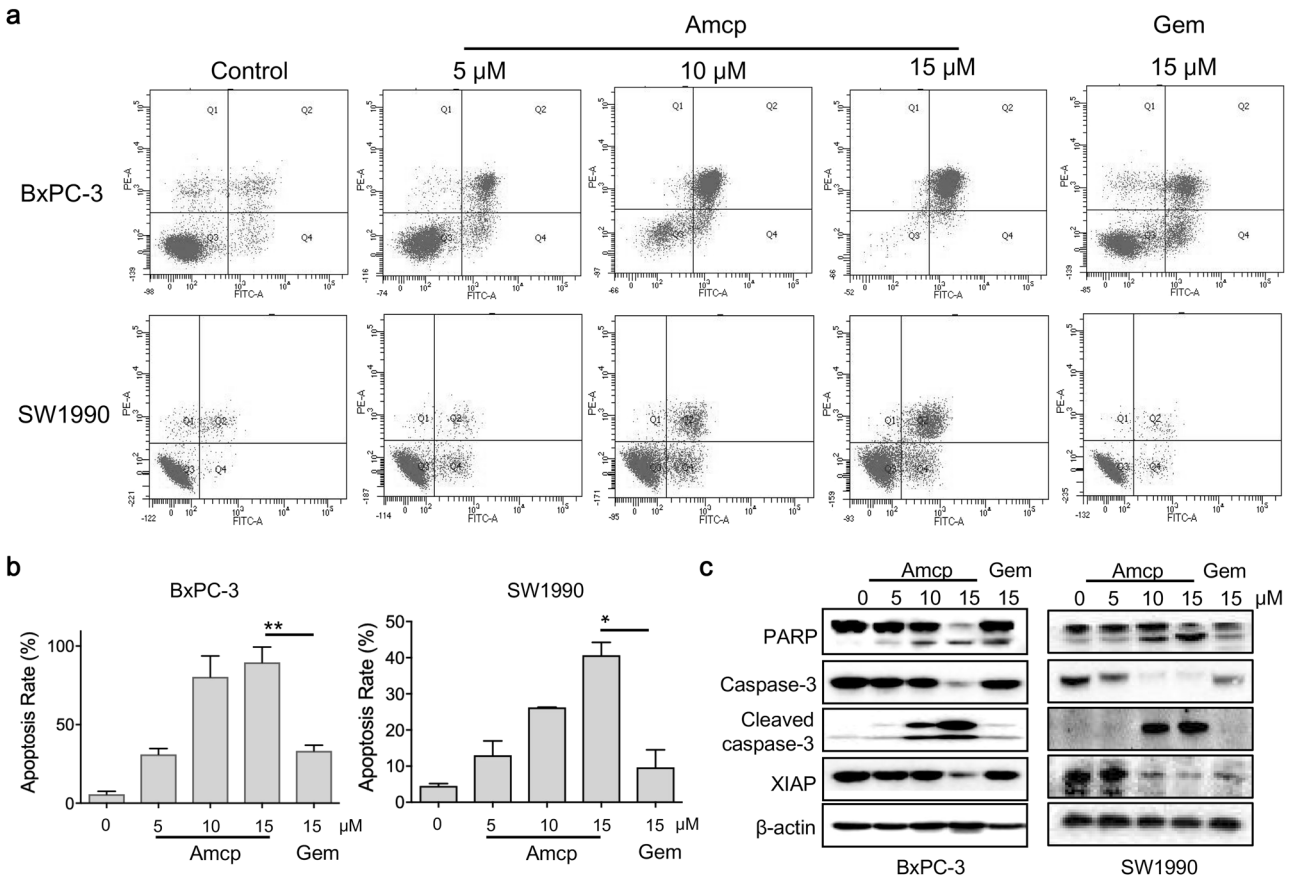


**Fig. 3 Amcp induced apoptosis in pancreatic cancer cells. a** Amcp induced apoptosis in BxPC-3 and SW1990 cells. Cells were treated with Amcp for 24 h before collection. Cells were then stained with Annexin V/PI and analyzed by flow cytometry. **b** Apoptotic cells were quantified by GraphPad Prism 5. **c** Cells were treated with Amcp or gemcitabine for 24 h before Western blotting assays. Three independent experiments were performed and the data were presented as the mean ± SD. $^{*}P < 0.05$, $^{**}P < 0.01$.

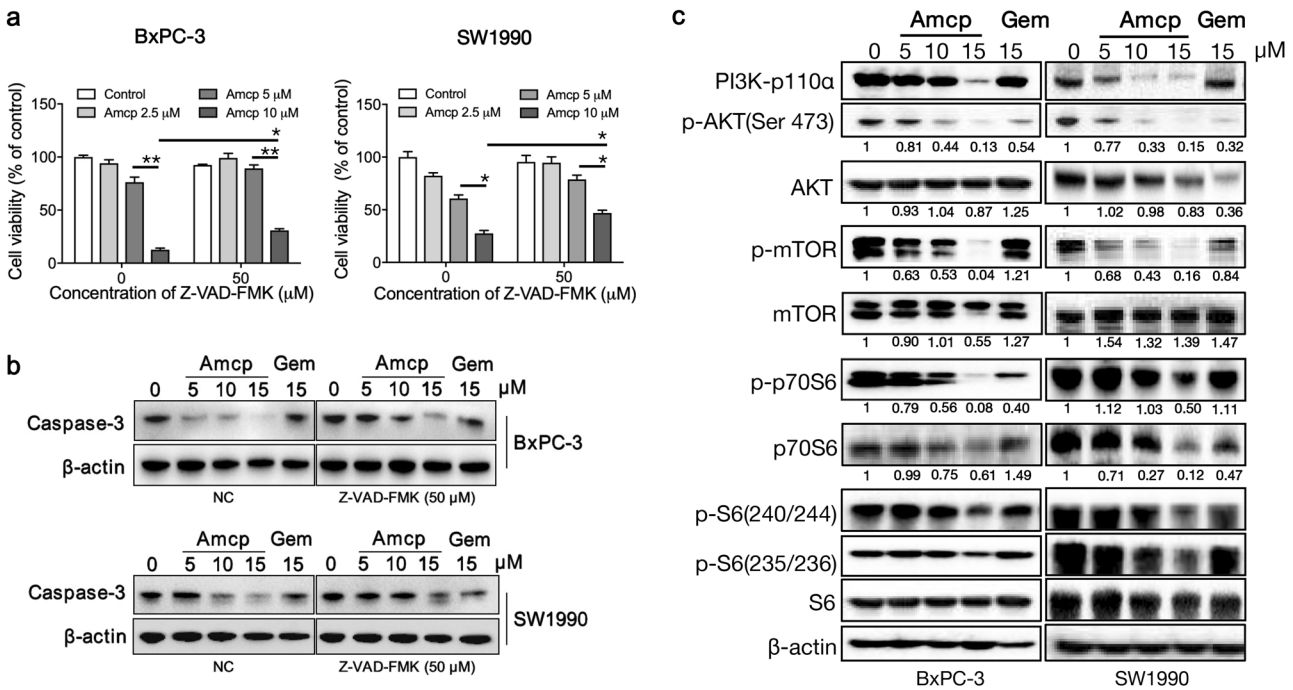


**Fig. 4 Amcp activated PI3K/AKT-regulated apoptotic proteins. a** Cells were pretreated with the indicated concentrations of Z-VAD-FMK for 4 h and then cultured with various concentrations of Amcp for another 24 h before the CCK-8 cell viability assay. **b** Caspase-3 levels in cells were examined with or without the presence of Z-VAD-FMK, followed by 24 h of treatment with Amcp or gemcitabine (Gem). **c** Cells were treated with the indicated concentrations of Amcp or gemcitabine for 24 h before Western blotting assays. The protein bands were visualized by an ECL system and analyzed using Bio-Rad Laboratories Quantity One software. $^{*}P < 0.05$, $^{**}P < 0.01$.

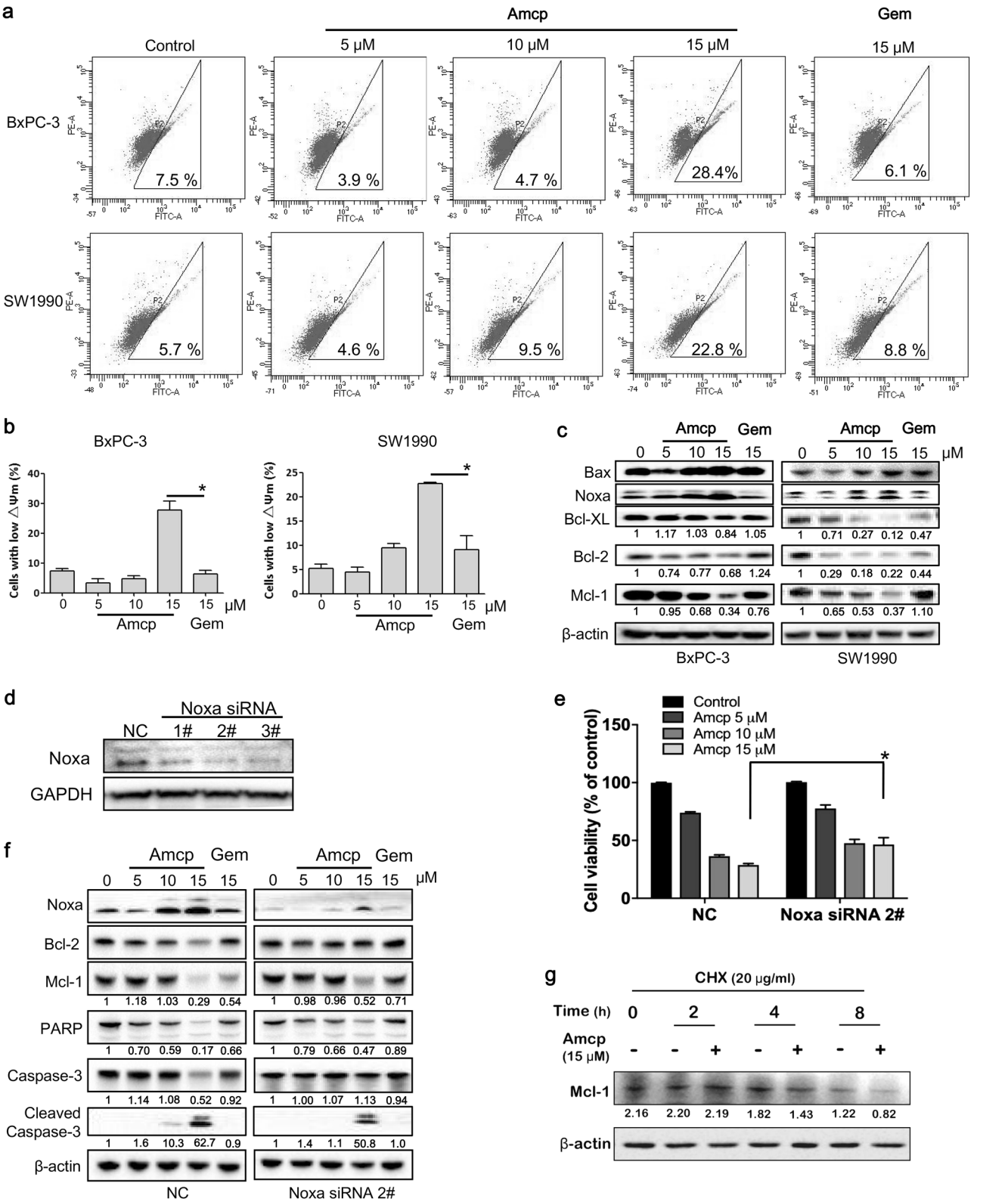


**Fig. 5 Amcp disrupted the mitochondrial membrane potential and affected mitochondrial proteins. a** BxPC-3 and SW1990 cells were seeded into six-well plates at a density of $2 \times 10^5$/well and were cultured for 24 h. After treatment with Amcp for 12 h, JC-1 staining was used to observe the depolarized mitochondrial membrane potential. Cells were analyzed by flow cytometry. **b** Quantitative analysis of cells with a depolarized mitochondria membrane. **c** Cells were treated with the indicated concentrations of Amcp or gemcitabine (Gem) for 24 h before Western blotting assays. *$P < 0.05$. **d** The protein level of Noxa was dramatically reduced by Noxa siRNA knockdown in BxPC-3 cells. **e** BxPC-3 cells were exposed to Amcp for 24 h with or without Noxa knockdown. Cell viability was determined by CCK-8 assays. **f** Noxa was knocked down by siRNA in BxPC-3 cells before treatment and cells were exposed to the indicated concentrations of Amcp or gemcitabine for 24 h before Western blotting analysis. **g** BxPC-3 cells were pretreated with 20 μg/mL cycloheximide (CHX) for 0.5 h and incubated with 15 μM Amcp for 2, 4, or 8 h. The Mcl-1 protein level was examined and quantitative analysis was performed using ImageJ 1.52q software (National Institute of Health, USA). *$P < 0.05$.

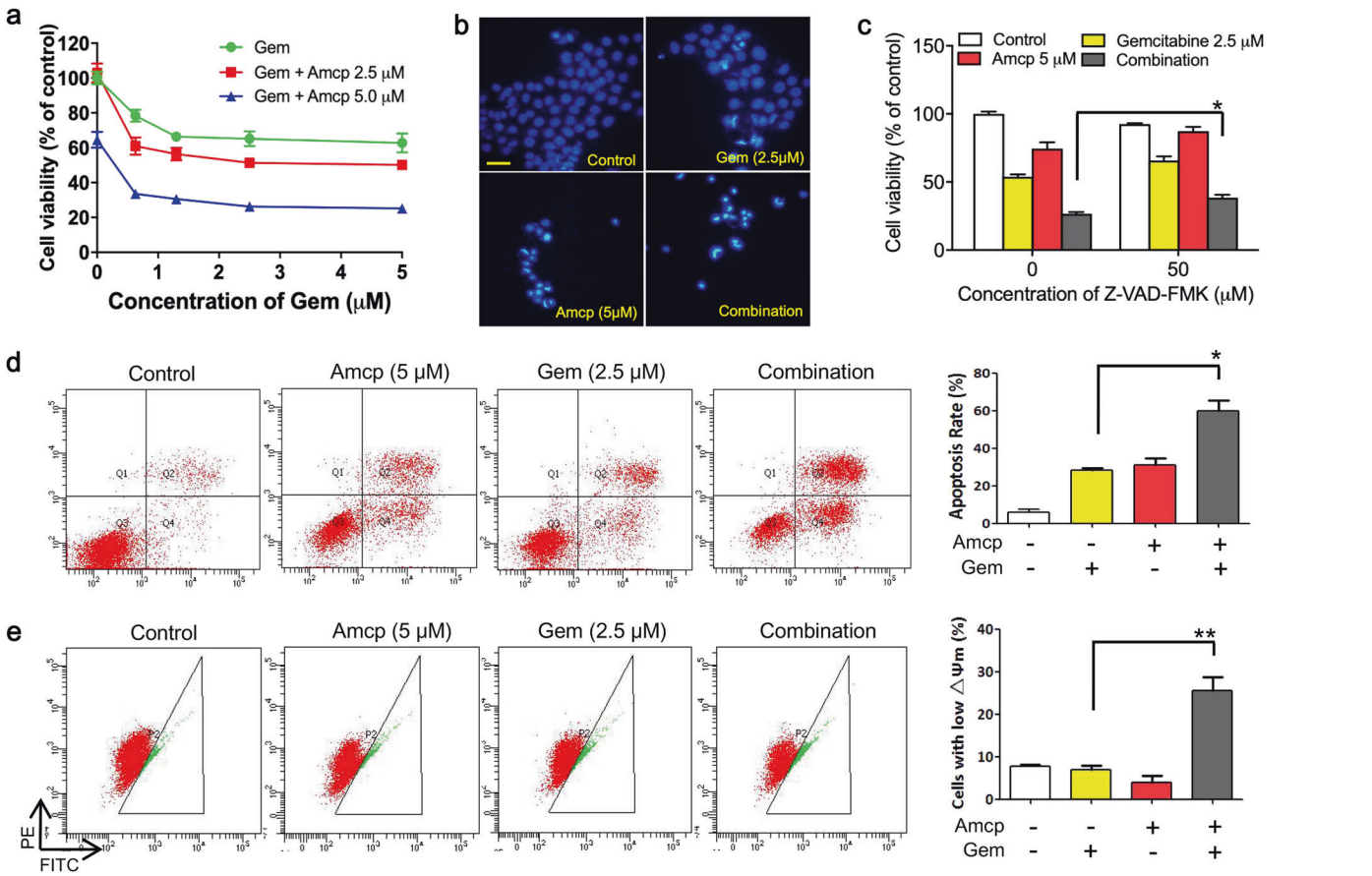


**Fig. 6 The combination of Amcp and gemcitabine synergistically induced apoptosis in BxPC-3 cells. a** BxPC-3 cells were treated with 0.625, 1.25, 2.5, or 5 μM gemcitabine (Gem) alone or in combination with 2.5 or 5.0 μM Amcp for 24 h before the CCK-8 assay. **b** DAPI staining was used to visualize the cell nucleus after treatment with gemcitabine, Amcp, or a combination of both for 24 h. **c** BxPC-3 cells were pretreated with Z-VAD-FMK for 4 h before exposure to gemcitabine, Amcp, or a combination of both. Cell viability was determined by CCK-8 assays after 24 h of treatment. **d** BxPC-3 cells were treated with gemcitabine, Amcp, or a combination of both for 24 h before collection. Cells were then stained with Annexin V/PI and analyzed by flow cytometry. **e** After treatment with gemcitabine, Amcp, or a combination of both for 12 h, JC-1 was used to measure the depolarization of the mitochondria membrane and BxPC-3 cells were then analyzed by flow cytometry. Scale bar = 20 μm. $^{*}P < 0.05$, $^{**}P < 0.01$.

phosphorylation of AKT is required for the full activation of Akt [26, 27]. We determined the inhibitory effects of Amcp on the PI3K/AKT pathway and found that 15 μM of Amcp obviously repressed the phosphorylation of AKT at S473. Meanwhile, the phosphorylation of downstream proteins, such as mTOR and p70S6 kinase, were substantially suppressed compared with that observed in cells treated with the same concentration of gemcitabine. Furthermore, Amcp treatment caused depolarization of the mitochondrial membrane, which was possibly attributed to the downregulation of Mcl-1 and the increased level of Noxa (Fig. 5) [28]. In fact, dual inhibition of mTOR and Mcl-1 has been reported to show unique advantages in cancer therapy and PI3K inhibition was observed to downregulate Mcl-1 [29, 30]. Noxa acts as an E3 ligase that can colocalize and associate with Mcl-1, resulting in the proteasomal degradation of Mcl-1 [31]. By knocking down Noxa, the number of viable cells increased from 25% to 48% during exposure to Amcp. In addition, the degradation of Mcl-1 was clearly accelerated after Amcp treatment, suggesting that Noxa-mediated Mcl-1 degradation was essential to Amcp-induced apoptosis (Fig. 5). Therefore, Amcp was capable of reducing the protein level of Mcl-1 by increasing its degradation.

In this study, we identified a novel derivative of valepotriate (denoted as Amcp) via a similarity search. Amcp showed potent anticancer activity against pancreatic cancer cells through the inhibition of the Mcl-1 and PI3K/AKT pathways, thereby stimulating caspase-dependent apoptosis. Moreover, Amcp had a synergistic effect when combined with gemcitabine. Therefore, our work not only suggests that Amcp is a promising dual-inhibitory anticancer agent but also highlights the importance of the further development of bioactive valepotriate derivatives.

## ACKNOWLEDGEMENTS

This study was supported by Key Laboratory of Clinical Cancer Pharmacology and Toxicology Research of Zhejiang Province, the Hangzhou Major Science and Technology Project (20172016A01), the Clinical Pharmacy of Zhejiang Key Medical Disciplines (2018-2-3), the Clinical Pharmacy of Hangzhou Key Medical Disciplines (2017-68-7), the Zhejiang Provincial Program for the Cultivation of High-level Innovative Health Talent (2010-190-4, NL), and the Natural Science Foundation of Zhejiang Province (LY20H310005, LY19H310004, and LY19H300001).

## AUTHOR CONTRIBUTIONS

NML and BZ designed the experiments and wrote the manuscript. YYY and KYS performed immunoblotting and flow cytometry experiments. FT performed the cytotoxicity experiments. JC and JXC performed the similarity search. XWD analyzed the data.

## ADDITIONAL INFORMATION

**Conflict of interest:** The authors declare no conflicts of interest.

## REFERENCES

1. Dreyer SB, Chang DK, Bailey P, Biankin AV. Pancreatic cancer genomes: implications for clinical management and therapeutic development. Clin Cancer Res. 2017;23:1638–46.
2. Amrutkar M, Gladhaug IP. Pancreatic cancer chemoresistance to gemcitabine. Cancers (Basel). 2017;9:E157.
3. Emmanouilidi A, Fyffe CA, Ferro R, Edling CE, Capone E, Sestito S, et al. Preclinical validation of 3-phosphoinositide-dependent protein kinase 1 inhibition in pancreatic cancer. J Exp Clin Cancer Res. 2019;38:191.
4. Bharadwaj U, Marin-Muller C, Li M, Chen C, Yao Q. Mesothelin confers pancreatic cancer cell resistance to TNF-alpha-induced apoptosis through Akt/PI3K/NF-kappaB activation and IL-6/Mcl-1 overexpression. Mol Cancer 2011;10:106.
5. Kour S, Rana S, Contreras JI, King HM, Robb CM, Sonawane YA, et al. CDK5 inhibitor downregulates Mcl-1 and sensitizes pancreatic cancer cell lines to Navitoclax. Mol Pharmacol 2019;96:419–29.
6. Zhang H, Hylander BL, LeVea C, Repasky EA, Straubinger RM, Adjei AA, et al. Enhanced FGFR signalling predisposes pancreatic cancer to the effect of a potent FGFR inhibitor in preclinical models. Br J Cancer. 2014;110:320–9.
7. Hedir S, De Giorgi M, Fogha J, De Pascale M, Weiswald LB, Brotin E, et al. Structure-guided design of pyridoclax derivatives based on Noxa/Mcl-1 interaction mode. Eur J Med Chem. 2018;159:357–80.
8. Tong J, Zheng X, Tan X, Fletcher R, Nikolovska-Coleska Z, Yu J, et al. Mcl-1 phosphorylation without degradation mediates sensitivity to HDAC inhibitors by liberating BH3-only proteins. Cancer Res 2018;78:4704–15.
9. Neoptolemos JP, Kleeff J, Michl P, Costello E, Greenhalf W, Palmer DH. Therapeutic developments in pancreatic cancer: current and future perspectives. Nat Rev Gastroenterol Hepatol. 2018;15:333–48.
10. Kirmizibekmez H, Kusz N, Berdi P, Zupko I, Hohmann J. New iridoids from the roots of *Valeriana dioscoridis* Sm. Fitoterapia 2018;130:73–8.
11. Liu YH, Wu PQ, Hu QL, Pei YJ, Qi FM, Zhan ZX, et al. Cytotoxic and antibacterial activities of iridoids and sesquiterpenoids from *Valeriana jatamansi*. Fitoterapia 2017;123:73–8.
12. Dong FW, Wu ZK, Yang L, Zi CT, Yang D, Ma RJ, et al. Iridoids and sesquiterpenoids of *Valeriana stenoptera* and their effects on NGF-induced neurite outgrowth in PC12 cells. Phytochemistry 2015;118:51–60.
13. Sun Y, Lan M, Chen X, Dai YL, Zhao XQ, Wang LW, et al. Anti-invasion and anti-metastasis effects of Valjatrate E via reduction of matrix metalloproteinases expression and suppression of MAPK/ERK signaling pathway. Biomed Pharmacother 2018;104:817–24.
14. Yang B, Zhu R, Tian SS, Wang YQ, Lou SY, Zhao HJ. Jatamanvaltrate P induces cell cycle arrest, apoptosis and autophagy in human breast cancer cells in vitro and in vivo. Biomed Pharmacother 2017;89:1027–36.
15. Conway JR, Herrmann D, Evans TJ, Morton JP, Timpson P. Combating pancreatic cancer with PI3K pathway inhibitors in the era of personalised medicine. Gut 2019;68:742–58.
16. Bean GR, Ganesan YT, Dong Y, Takeda S, Liu H, Chan PM, et al. PUMA and BIM are required for oncogene inactivation-induced apoptosis. Sci Signal 2013;6:ra20.
17. Leverson JD, Sampath D, Souers AJ, Rosenberg SH, Fairbrother WJ, Amiot M, et al. Found in translation: How preclinical research is guiding the clinical development of the BCL2-selective inhibitor Venetoclax. Cancer Disco. 2017;7:1376–93.
18. Tan YZ, Peng C, Hu CJ, Li HX, Li WB, He JL, et al. Iridoids from *Valeriana jatamansi* induce autophagy-associated cell death via the PDK1/Akt/mTOR pathway in HCT116 human colorectal carcinoma cells. Bioorg Chem 2019;87:136–41.
19. de Avila JM, Pereira AO, Zachow LL, Gehm AZ, Santos MZ, Mostardeiro MA, et al. Chemical constituents from *Valeriana* polystachya Smith and evaluation of their effects on the acetylcholinesterase and prolyl oligopeptidase activities. Fitoterapia 2018;131:80–5.
20. Dong FW, Jiang HH, Yang L, Gong Y, Zi CT, Yang D, et al. Valepotriates from the roots and rhizomes of *Valeriana jatamansi* Jones as novel N-type calcium channel antagonists. Front Pharmacol 2018;9:885.
21. Guo Z, Guozhang H, Wang H, Li Z, Liu N. Ampelopsin inhibits human glioma through inducing apoptosis and autophagy dependent on ROS generation and JNK pathway. Biomed Pharmacother 2019;116:108524.
22. Li H, Gao X, Huang X, Wang X, Xu S, Uchita T, et al. Hydrogen sulfide donating ent-kaurane and spirolactone-type 6,7-seco-ent-kaurane derivatives: design, synthesis and antiproliferative properties. Eur J Med Chem. 2019;178:446–57.
23. Kim KY, Hwang SK, Park SY, Kim MJ, Jun DY, Kim YH. l-Serine protects mouse hippocampal neuronal HT22cells against oxidative stress-mediated mitochondrial damage and apoptotic cell death. Free Radic Biol Med. 2019;141:447–60.
24. Denault JB, Eckelman BP, Shin H, Pop C, Salvesen GS. Caspase 3 attenuates XIAP (X-linked inhibitor of apoptosis protein)-mediated inhibition of caspase 9. Biochem J. 2007;405:11–9.
25. Yoo JK, Lee JM, Kang SH, Jeon SH, Kim CM, Oh SH, et al. The novel microRNA hsa-miR-CHA1 regulates cell proliferation and apoptosis in human lung cancer by targeting XIAP. Lung Cancer 2019;132:99–106.
26. Zhang H, Pan YZ, Cheung M, Cao M, Yu C, Chen L, et al. LAMB3 mediates apoptotic, proliferative, invasive, and metastatic behaviors in pancreatic cancer by regulating the PI3K/Akt signaling pathway. Cell Death Dis. 2019;10:230.
27. Fu XH, Zhang X, Yang H, Xu XW, Hu ZL, Yan J, et al. CUDC-907 displays potent antitumor activity against human pancreatic adenocarcinoma in vitro and in vivo through inhibition of HDAC6 to downregulate c-Myc expression. Acta Pharmacol Sin. 2019;40:677–88.
28. Zhao H, Ma Y, Zhang L. Low-molecular-mass hyaluronan induces pulmonary inflammation by up-regulation of Mcl-1 to inhibit neutrophil apoptosis via PI3K/Akt1 pathway. Immunology 2018;155:387–95.
29. Bojarczuk K, Sasi BK, Gobessi S, Innocenti I, Pozzato G, Laurenti L, et al. BCR signaling inhibitors differ in their ability to overcome Mcl-1-mediated resistance of CLL B cells to ABT-199. Blood 2016;127:3192–201.
30. Bojarczuk K, Wienand K, Ryan JA, Chen L, Villalobos-Ortiz M, Mandato E, et al. Targeted inhibition of PI3Kalpha/delta is synergistic with BCL-2 blockade in genetically defined subtypes of DLBCL. Blood 2019;133:70–80.
31. Kim EY, Sudini K, Singh AK, Haque M, Leaman D, Khuder S, et al. Ursolic acid facilitates apoptosis in rheumatoid arthritis synovial fibroblasts by inducing SP1-mediated Noxa expression and proteasomal degradation of Mcl-1. FASEB J. 2018; fj201800425R.